Topological configurations of principal network-forming clusters in As/Ge-Se glasses

M. HYLA[a], O. SHPOTYUK[a,b,*]

[a]*Institute of Physics, Faculty of Mathematics and Natural Science, Jan Dlugosz University of Czestochowa, 13/15, al. Armii Krajowej, Czestochowa, 42-200,Poland*
[b]*Vlokh Institute of Physical Optics 23, Dragomanov str., Lviv, 79005, Ukraine*

Quantum chemical *ab initio* calculations with RHF/6-311G[*] basis set are performed employing cation-interlinking network cluster approach (CINCA) to compare topological configurations of principal network-forming clusters possible in binary trigonal-type As-Se and tetragonal-type Ge-Se glass-forming systems. Geometrically optimized configurations and mean forming energies are computed for two-cation clusters involved corner-, edge- and face-shared interlinking between neighbouring structural units composing these glasses. It is shown that corner-sharing configurations with one common atom in direct inter-cluster bridge are evidently preferential for $AsSe_{3/2}$ pyramids in As-Se glasses, while corner- and edge-sharing configurations (with one and two common Se atoms, respectively) are almost equivalent in their forming energies for $GeSe_{4/2}$ tetrahedra in Ge-Se glasses. This effect is ascribed to principal difference in bond-angular distortions within cluster cores corresponding to interlinked pyramidal $AsSe_{3/2}$ and tetrahedral $GeSe_{4/2}$ building blocks in a glassy network.

1. Introduction

Covalent-bonded compounds of chalcogen family of group VI elements of the periodic table (S, Se or Te) with pnictogens (commonly As, sometimes Sb or Bi) and/or tathogens (mainly Ge, more rarely Si) known also as chalcogenide glasses (ChG) [1-3] have attracted a high interest in modern glass-science community because of promising perspectives on their widespread application in IR optics and photonics [4-6]. Nevertheless, despite scrupulous theoretical and experimental research in last decades, these disordered materials still possess a number of features needed deeper understanding, such as strict correlation between atomic structure and physical properties, especially in view of recent achievements in their nanostructurization technology exploring extra-small interatomic length-scales [7-9].

In a general opinion, the ChG possess disordered networks with fully-saturated covalent bonds, which differ essentially from crystallographic-ordered lattices of their crystalline counterparts by lacking of long-range inter-atomic ordering [1,2]. Owing to short-range order in the nearest atomic arrangement, resulting from some coordination polyhedrons like $AsSe_{3/2}$ pyramids or $GeSe_{4/2}$ tetrahedra, the ChG reveal typical semiconductor trends in their optical and electrical properties [1-3].

According to one of most popular structural insight, the *chain crossing* (CC) model [10-12], these coordination polyhedrons are randomly cross-linked through chalcogen atoms (e.g. variable-length chalcogen chains in dependence on ChG composition), forming in such a way the characteristic corner-sharing (CS) bridges, where only one atom or short chain composed of a few sequent chalcogen atoms is common between two neighboring polyhedrons. This structural model is proper for binary As-Se ChG built of trigonal $AsSe_{3/2}$ pyramids [1,2,10]. Despite some exceptions concerning restrictions in the distribution of –Se– bridging links between these $AsSe_{3/2}$ pyramids [13-15], the CC network-forming rules dominate preferentially in Se-rich ChG.

In other insight, the molecular-like atomic entities such as *outrigger raft* (ORR) motives [16] form a competitive input to CC Se-bridging network-forming trend. This structural organization is character for tetragonal-type networks of Ge-Se ChG built of $GeSe_{4/2}$ tetrahedrons, which demonstrate specific *pseudo-self-adaptability* phenomenon (identifying covalent bonds through mechanical Lagrangian constraints of freedom) in the range from 40 to 52 at. % of Ge [17-20]. These ChG contain extended ORR clusters consisting centroid of two edge-sharing (ES) $GeSe_{4/2}$ tetrahedra linked through two common Se atoms, surrounded by four CS $GeSe_{4/2}$ tetrahedra (linked via one common Se atom) [21], which are topologically stressed-rigid in view of available constraints n_c exceeding a space dimensionality D=3. Noteworthy that in respect to Phillips-Thorpe rigidity theory [22,23], the glass-forming network is considered to be optimal under the same number of constraints n_c and degrees of freedom D. Such multiply interlinked ORR configurations are typical to β-GeS_2, forming basic motive of this crystalline phase [16,24]. Similar over-constrained atomic fragments in Ge-Se ChG, interconnected by bridging $\equiv$Ge-Se-Se-Ge$\equiv$ links, which are optimally-constrained having n_c=3, create an illusion of optimal

(rigid but stressed-free) glassy network, thus termed in [17-20] as *quasi-adaptive intermediate phase.*

What is a reason for such essential difference in the network-forming tendencies in these trigonal-type As-Se and tetragonal-type Ge-Se ChG?

In this work, we shall answer this question exploring quantum chemical *ab initio* calculation within previously developed *cation-interlinking network cluster approach* (CINCA) [25,26] for principal topological configurations (CS, ES and even face-sharing – FS) possible between primary glass-forming polyhedrons in these ChG.

2. Structural models and energy calculations for chalcogenide glasses

Regardless of accepted glass formation model (CC or molecular clustering), the glassy network can be built of some atomic blocks forming *primary cation-centered polyhedrons*, these being $AsSe_{3/2}$ pyramids and $GeSe_{4/2}$ tetrahedrons (Fig. 1) for As-Se and Ge-Se, respectively.

(a)   (b)
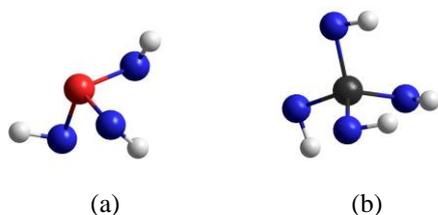
Fig. 1. Geometrically optimized configurations of single $AsSe_{3/2}$ pyramid (a) and $GeSe_{4/2}$ tetrahedron (b) composing binary As-Se and Ge-Se ChG (the As, Ge and Se atoms are respectively red-, black- and blue-colored, the terminated H atoms are shown by grey circles)

In dependence on composition, the glass structure can be reproduced via some *network-forming clusters* (NFC), composed of these polyhedrons surrounded by outer chalcogen *shell*, owing to their multiple repetition in a glassy network, like as elementary unit cells in a crystalline lattice [25-27]. In the case of shortest interlinking through common chalcogen atom, the NFC comprises most essential interaction between polyhedrons, thus transforming to *base* or *principal* NFC. This principal NFC, because of the same CS-linking for outer chalcogen environment, reflects specificity of direct interaction between primary cation-centered polyhedrons, thus defining preferential type of glass forming in ChG (network CC or molecular clustering).

Thereby, in ChG of binary As-Se and/or Ge-Se systems, the highly coordinated cation-like atoms (such as As or Ge) form *primary cation-centered polyhedrons* (e.g. $AsSe_{3/2}$ pyramids or $GeSe_{4/2}$ tetrahedrons, respectively, as it shown in Fig. 1) in preferentially two-fold coordinated anion-like chalcogen environment (S, Se or Te atoms). These polyhedrons compose *principal* NFC of different topological configurations by direct interlinking through one (CS), two (ES) or three (FS) common chalcogen atoms (as it shown in Fig. 2), which undoubtedly depends

on a specificity of chemical interaction between neighboring polyhedrons (*intra-cluster* interaction).

(a)   (d)

(b)   (e)

(c)   (f)
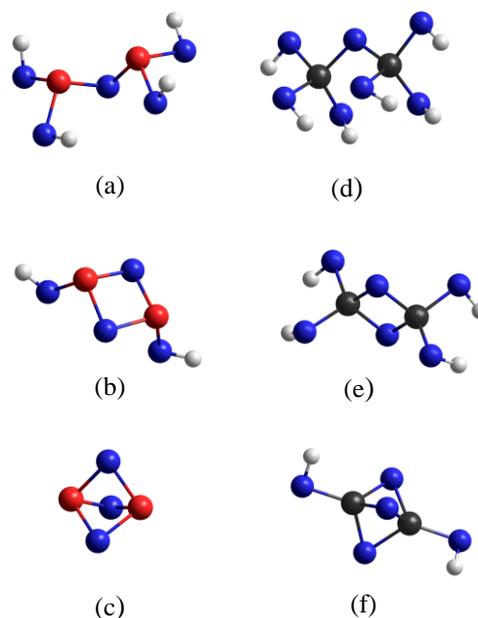
Fig. 2. Geometrically optimized configurations of CS (a,d), ES (b,e) and FS (c,f) NFC configurations possible in As-Se (a,b,c) and Ge-Se (d,e,f) ChG (the As, Ge and Se atoms are red-, black- and blue-colored, respectively, the terminated H atoms are shown by grey circles)

Efficient numerical criterion for governing glass-forming tendency of the chosen ChG can be developed at the basis of energy calculations for corresponding principal NFC (schematic view of NFC based on CS and ES configurations of $AsSe_{3/2}$ pyramids and $GeSe_{4/2}$ tetrahedra showing intra-cluster cores is given in Fig. 3).

(a)   (b)

(c)   (d)
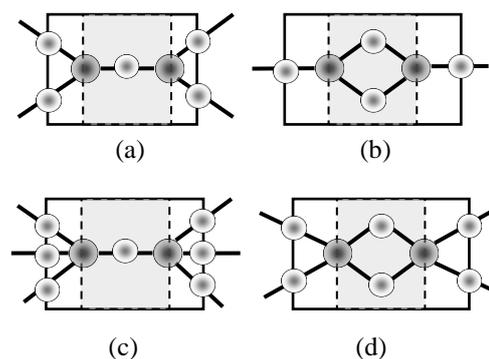
Fig. 3. Schematic view of $AsSe_{3/2}$ pyramids (a,b) and $GeSe_{4/2}$ tetrahedrons (c,d) forming principal CS (a,c) and ES (b,d) NFC in As-Se and Ge-Se glasses. The respective $As_{2/3}Se$ (a), $As_{4/3}Se_2$ (b), $Ge_{1/2}Se$ (c) and Ge_2Se_4 (d) intra-cluster cores are depicted by grey-colored rectangles

We start our cluster modeling with energy computing for geometrically optimized single polyhedrons, i.e. trigonal $AsSe_{3/2}$ pyramids and $GeSe_{4/2}$ tetrahedrons (see Fig. 1), accepted them as primary structural blocks

composing ChG of binary As-Se and Ge-Se systems. This simulation serves as reference point in the further NFC modeling with CINCA algorithm [25,26].

Then, three principal topological configurations based on CS, ES and FS linking between neighboring $AsSe_{3/2}$ and $GeSe_{4/2}$ polyhedrons (see Fig. 2) will be analyzed.

Instead of complicated and time-consuming modeling procedures for glassy networks usually evolved hundreds or even thousands of atoms [28-31], the CINCA algorithm allows more simplified simulation route for relatively small NFC using available PC software like HyperChem Release 7.5 program [25,26]. The quantum-chemical *ab-initio* calculations are performed with restricted Hartree-Fock (RHF) self-consistent field method using split-valence double-zeta basis set with single polarization function $6\text{-}311G^*$ [32,33]. The final geometrical optimization and single point energy calculations are carried out employing Fletcher-Reeves conjugate gradient method until 0.1 kcal/Å·mol root-mean-square gradient is reached. The molecular-like configurations of NFC are reconstructed in respect to "8-N" rule, required to all boundary Se atoms belonging to two neighboring polyhedrons be terminated by hydrogen H atoms (grey-colored circles in Fig. 1 and 2). Therefore, the finalized *cluster formation energy* (CFE) after subtraction the energy of all atoms are corrected on both hydrogen atoms and –Se–H bond energies.

These CFE values will be taken to compare different principal configurations of NFC built of two CS-, ES- and FS-linked polyhedrons, the energy of single polyhedron serving as reference point in this comparison. For As-Se ChG, this reference is trigonal $AsSe_{3/2}$ pyramid (Fig. 1a) having three shared Se atoms with neighbors of the same type, the CFE reaching -72.309 kcal/mol. In case of Ge-Se ChG, this is single $GeSe_{4/2}$ tetrahedron (Fig. 1b), having four CS-linked Se atoms with the same neighbors, the CFE reaching -87.029 kcal/mol. These CFE are further taken to normalize the calculated energies of principal NFC and corresponding *intra-cluster cores*, determined them as *respective* CFE E_f, e.g. mean CFE in respect to the energy of single $AsSe_{3/2}$ pyramid or $GeSe_{4/2}$ tetrahedron.

3. Results and discussion

The computed geometrically-optimized configurations of principal NFC in ChG of As-Se and Ge-Se systems are shown in Fig. 2. The values of bond distances and angles for CS-, ES- and FS-configurations along with ones for $AsSe_{3/2}$ pyramid (Fig. 1a) are given in Table 1. Similarly, the geometrically-optimized parameters for CS-, ES- and FS-linked $GeSe_{4/2}$ tetrahedrons are given in Table 2, and calculated values of respective CFE for these NFC and corresponding intra-cluster cores are gathered in Table 3.

In case of As-Se ChG, we deal with two CS $AsSe_{3/2}$ pyramids forming As_2Se_3 NFC (Fig. 2a), having $As_{2/3}Se$ intra-cluster core (Fig. 3a). Mean CFE of this CS-As_2Se_3 NFC (-72.619 kcal/mol) corresponds to E_f=0.31 kcal/mol (e.g. value of CFE recalculated in respect to the energy of single $AsSe_{3/2}$ pyramid). In a similar way, the value of

respective E_f=0.93 kcal/mol is obtained for $As_{2/3}Se$ intra-cluster core of this NFC (the positive energy means this cluster is energetically favored in respect to single $AsSe_{3/2}$ pyramid, so the CS inter-cluster configuration seems most stable in As-Se ChG). Noteworthy, both CS-As_2Se_3 NFC and corresponding $As_{2/3}Se$ intra-cluster core possess optimal number of constraints per atom n_c approaching space dimensionality D=3.

Table 1. Parameters of geometrically-optimized atomic clusters in binary As-Se ChG system: single-$AsSe_{3/2}$ pyramid, CS-As_2Se_3, ES-As_2Se_3 and FS-As_2Se_3.

Cluster	Bond distance [$\cdot 10^{-4}$ nm]	Bond angle [deg]	
	As-Se	$\angle$Se-As-Se	$\angle$As-Se-As
$AsSe_{3/2}$-single	2393	103.3	-
	2397	102.6	
	2399	93.9	
average	*2396*	*99.9*	*-*
As_2Se_3-CS	2398	102.8	95.9
	2391	100.2	
	2415	93.2	
	2400	97.4	
	2398	97.5	
	2396	98.7	
average	*2400*	*98.3*	*95.9*
As_2Se_3-ES	2391	102.2	89.7
	2410	101.6	89.7
	2408	89.2	
	2407	89.2	
	2410	101.6	
	2391	102.2	
average	*2403*	*97.7*	*89.7*
As_2Se_3-FS	2428	87.7	73.8
	2428	87.7	73.8
	2428	87.7	73.8
	2428	87.7	
	2428	87.7	
	2429	87.7	
average	*2428*	*87.7*	*73.8*

The next of network-forming atomic configurations is ES-As_2Se_3 NFC built of two ES $AsSe_{3/2}$ pyramids (see Fig. 2b) with $As_{4/3}Se_2$ intra-cluster core (see Fig. 3b), the CFE being reduced to -0.81 kcal/mol and -1.22 kcal/mol, respectively. These under-constrained entities (in view of n_c reduced to 2.60 and 2.40 for NFC and intra-cluster core, respectively) possess additional floppy modes due to small ring (quadrangle) evolved.

Other possibility is FS-As_2Se_3 NFC having three common Se atoms in bridge between two neighboring $AsSe_{3/2}$ trigonal pyramids (Fig. 2c) with iso-compositional As_2Se_3 inter-cluster core, both NFC and corresponding core possessing the same but highly reduced respective average energy E_f=-4.61 kcal/mol and averaged number of constraints per atom n_c=2.20 (due to two triangles evolved).

Thus, in respect to the above calculations (Table 3), the CS-As_2Se_3 NFC seems most suitable to reproduce the governing glass-forming tendencies in binary As-Se ChG, this being defined by energetic (in view of respective CFE E_f) and topological (in view of optimal number of constraints per atom n_c) preference of $As_{2/3}Se$ intra-cluster core. Let's clarify correlation between calculated (Table 1) and experimental structural modes for known counterparts taken from this binary As-Se system.

In full respect to X-ray diffraction [34,35], the layer structure of orpiment-type As_2Se_3 crystal consists of *zigzag* almost trigonal equivalent chains built of CS-$AsSe_{3/2}$ pyramids (with average As-Se distance of 2.40 Å) interlinked via inter-chain Se-based angle close to 100°, while inter-chain ∠As-**Se**-As angle equals 85°. The latter is a signature of more extended structure, which cannot be reflected in our modeling because of length scale limited to two nearest cation-centered $AsSe_{3/2}$ pyramids (this feature is also undetectable in diffraction experiments on glassy As-Se [36,37]). Other angles in the structure of this As_2Se_3 crystal are based on As atoms (∠Se-**As**-Se), they being distributed in wide 91.8÷105.0° range with an averaged 98.4° value [34]. At the same time, the X-ray diffraction data of Renninger and Averbach [36] from series of glassy As-Se testify that first-neighbor correlation peak, which can be undoubtedly associated under these conditions with As-Se bond length, is placed at 2.408 Å for As_2Se_3. Other experiments with X-ray and neutron diffraction studies performed by Leadbetter and Apling [37] on As-Se glass gave nearest As-Se distance close to 2.44 Å and average 96.8° value for ∠Se-**As**-Se. It should be noted that As-Se bond length obtained directly from Pauling's covalent radii is 2.42 Å [38]. All these data correlate well with direct compositional study of chemical ordering in Se-rich As-Se glasses exploring high-resolution XPS [39], supported by recent free-volume void structure research with positron annihilation lifetime spectroscopy [40].

Although the NFC sizes in our modeling are rather limited and effects of environmental influences are entirely uncompleted, the computed bond distances and angles are in good coincidence with these experimental data, so justifying the computed geometry-optimized parameters. Thus, the lengths of heteronuclear As-Se bond in all atomic configurations of simulated NFC (Table 1) are well fitted to 2.391÷2.429 Å domain, giving in average 2.408 Å. The slightly longer bonds (the upper limit in this range) occur only in energetically unfavorable FS-As_2Se_3 configuration. The bond angles based on As atom neighboring with two Se atoms (∠Se-**As**-Se) in single $AsSe_{3/2}$ pyramid and energetically favorable CS-As_2Se_3 NFC are fitted to 93.2÷103.3° range (giving 98.8° in average) and bond angles based on Se atom (∠As-**Se**-As) is close to 95.9°.

But essential distortions are found in bond angles for ES-As_2Se_3 and FS-As_2Se_3 configurations (see Table 1). In case of ES-As_2Se_3, the intra-cluster core angles are around 89.2° for ∠Se-**As**-Se and 89.7° for ∠As-**Se**-As. At the same time, in case of FS-As_2Se_3, the intra-cluster core angles are more changed reaching 87.7° for ∠Se-**As**-Se and 73.8° for ∠As-**Se**-As. Thus, the computed bond

distances and angles in our structural models for As-Se ChG especially based on CS-As_2Se_3 NFC are in good agreement with known data. At the same time, angular distortions in intra-cluster cores of ES- and FS-NFC make them energetically unfavorable.

Table 2. Parameters of geometrically-optimized atomic clusters in binary Ge-Se ChG system: single-$GeSe_{4/2}$ tetrahedron, CS-Ge_2Se_4, ES-Ge_2Se_4 and FS-Ge_2Se_4

Cluster	Bond distance [·10^{-4} nm]	Bond angle [deg]	
	Ge-Se	∠Se-Ge-Se	∠Ge-Se-Ge
$GeSe_{4/2}$-single	2375	102.8	-
	2379	108.6	
	2379	108.6	
	2366	110.4	
		113.1	
		113.1	
average	*2375*	*109.4*	-
Ge_2Se_4-CS	2379	111.9	109.2
	2382	111.9	
	2382	110.6	
	2367	100.6	
	2396	110.7	
	2371	110.7	
	2371	107.3	
	2367	112.5	
		107.3	
		114.7	
		114.9	
		98.8	
average	*2377*	*109.3*	*109.2*
Ge_2Se_4-ES	2371	114.2	83.3
	2371	114.2	82.9
	2376	112.0	
	2385	109.2	
	2376	109.2	
	2386	96.9	
	2371	114.2	
	2371	114.2	
		112.0	
		109.2	
		109.2	
		96.9	
average	*2376*	*109.3*	*83.1*
Ge_2Se_4-FS	2343	120.9	66.2
	2416	123.9	66.3
	2424	124.6	66.3
	2404	93.2	
	2424	93.1	
	2404	92.7	
	2416	123.8	
	2343	120.9	
		124.6	
		92.7	
		93.1	
		93.2	
average	*2397*	*108.0*	*66.3*

In case of binary Ge-Se ChG, the main glass-forming structural unit is single $GeSe_{4/2}$ tetrahedron (see Fig. 1b). As it follows from Table 2, the length of Ge-Se covalent bond in this geometrically-optimized cation-centered polyhedron is well fitted to 2.366÷2.379 Å, and bond angles on Ge atom ($\angle$Se-**Ge**-Se) are compactly grouped around tetrahedral angle in a range of 102.8÷113.1°.

The computed parameters for Ge-Se ChG gathered in Table 2 will be compared with known experimental data for crystalline and amorphous counterparts in this system [41-50]. The crystalline structure of layered $GeSe_2$ is built of $GeSe_{4/2}$ tetrahedra linked by common corners or edges. In respect to X-ray diffraction for this crystal by Dittmar and Schäfer [41], the Ge-Se lengths change from 2.337 to 2.369 Å (2.355 Å in average), Ge-based $\angle$Se-**Ge**-Se angles change from 94.5° to 116° (109.30° in average) and Se-based $\angle$Ge-**Se**-Ge angle change from 80.2° to 100.1°. Neutron and high-energy synchrotron diffraction measurements on glassy $GeSe_2$ [42-46] show Ge-Se distance equals 2.36 Å and $\angle$Se-**Ge**-Se bond angle near ~105°. For $\angle$Ge-**Se**-Ge angles based on Se atom, two groups of values can be distinguished, the first being close to ~80° for ES-configuration and second being close to 98° for CS-configuration. Although crystalline GeSe has NaCl-type structure with partial ionicity [47,48], the X-ray diffraction data show that amorphous GeSe has Ge-Se covalent bonds of ~2.37 Å length [49]. The length of this Ge-Se bond in mechanically milled amorphous $GeSe_2$, Ge_3Se_4 and Ge_4Se_5 in respect to X-ray diffraction and EXAFS measurements [50] are well fitted to 0.235÷0.237 nm domain (0.236 nm in average).

Let's refer to geometrically-optimized principal NFC in this binary Ge-Se system shown on Fig. 2d,e,f.

Two CS $GeSe_{4/2}$ tetrahedra form CS-Ge_2Se_4 NFC (Fig. 2d) with $Ge_{1/2}$Se intra-cluster core (Fig. 3c). Both atomic entities are topologically over-constrained with n_c=3.67, that is far beyond dimensionality of space (D=3). The lengths of Ge-Se bonds are well fitted to 2.367÷2.382 Å domain (2.377 Å in average) and $\angle$Se-**Ge**-Se angles range from 98.8° to 114.9° (109.3° in average). Thus, the structural parameters of this configuration are in good agreement with ones proper to single $GeSe_{4/2}$ tetrahedron (Table 2). The $\angle$Ge-**Se**-Ge angle where Se atom is shared between two $GeSe_{4/2}$ tetrahedra equals 109.2°, which is in good agreement with data of Murakami et al. [45]. The respective CFE tends to -0.24 kcal/mol for CS-Ge_2Se_4 NFC and -0.98 kcal/mol for $Ge_{1/2}$Se intra-cluster core.

Two ES $GeSe_{4/2}$ tetrahedra form over-constrained (n_c=3.33) ES-Ge_2Se_4 NFC (Fig. 2e) having optimally-constrained (n_c=3.00) $GeSe_2$ intra-cluster core (Fig. 3d). The Ge-Se bond lengths corresponding to this configuration are in 2.371÷2.386 Å range (2.376 Å in average). The bond angles based on Ge atom neighboring with two Se atoms ($\angle$Se-**Ge**-Se) are well fitted in 96.9°-114.2° domain (109.3° in average). These parameters do not differ essentially from those, character for single $GeSe_{4/2}$ tetrahedron or CS-$GeSe_{4/2}$ NFC (Table 2). The values of two $\angle$Ge-**Se**-Ge bond angles, where Se atom is shared between two Ge atoms, are 83.3° and 82.9° (~83.1° in average). This is in good agreement with known data

for ES-Ge_2Se_4 configuration in this system [44,45]. The CFE for this NFC reaches -0.37 kcal/mol, thus being close to CFE of CS-Ge_2Se_4 NFC (see Table 2). Interestingly, the CFE for $GeSe_2$ intra-cluster core (-0.75 kcal/mol) is even better than for $Ge_{1/2}$Se core (-0.98 kcal/mol). Thus, in case of binary Ge-Se system, the energetic difference between CS-Ge_2Se_4 and ES-Ge_2Se_4 NFC is negligible, testifying in a favor of nearly equal possibilities for their appearance in a glassy network.

Table 3. Computed values of respective CFE E_f for different geometrically-optimized NFC and intra-cluster cores in ChG of As-Se and Ge-Se systems along with corresponding values of constraints per atom n_c

Cluster	NFC		intra-cluster core	
	n_c	E_f, [kcal/mol]	n_c	E_f, [kcal/mol]
CS-As$_2$Se$_3$	3.00	0.31	3.00	0.93
ES-As$_2$Se$_3$	2.60	-0.81	2.40	-1.22
Fs-As$_2$Se$_3$	2.20	-4.61	2.20	-4.61
CS-Ge$_2$Se$_4$	3.67	-0.24	3.67	-0.98
ES-Ge$_2$Se$_4$	3.33	-0.37	3.00	-0.75
FS-Ge$_2$Se$_4$	3.00	-6.31	2.78	-8.42

The FS $GeSe_{4/2}$ tetrahedras forming optimally-constrained (n_c=3.00) FS-Ge_2Se_4 NFC (Fig. 2f) with under-constrained (n_c=2.78) $Ge_{3/2}Se_2$ inter-cluster core are rather impossible in Ge-Se ChG because of unfavorable CFE in Table 3 (E_f=-6.31 kcal/mol for NFC and -8.42 kcal/mol for inter-cluster core). The lengths of Ge-Se bonds are fitted to 2.343÷2.424 Å range (2.397 Å in average). In contrast to equally-possible CS- and ES-configurations both having $\angle$Se-**Ge**-Se bond angles close to ~109°, the FS-Ge_2Se_4 NFC contains comparable proportions of these two angles grouped near 93° and 120.9°÷124.6°, while $\angle$Ge-**Se**-Ge tends to unrealistically low 66.3°. It seems that this FS-configuration is not favored because of huge distortions in bond lengths and angles, preferentially within intra-cluster $Ge_{3/2}Se_2$ core.

Thus, both types of NFC in CS- and ES-configurations play an approximately equivalent role in the glass-forming ability of binary Ge-Se ChG. By changing glass composition within this system, the tight interconnection between CS and ES structural blocks governs main network-forming tendency as transition from CC model of uniformly-distributed cation-centered polyhedrons (like CS-As$_2$Se$_3$ NFC in As-Se glass) towards molecular-cluster ORR model of competitive CS-ES polyhedrons (like CS-Ge_2Se_4 and ES-Ge_2Se_4 NFC in binary Ge-Se glass). Topological configuration of intra-cluster core is rather responsible for energetically favorable glass-forming trends in both As-Se and Ge-Se glassy systems. Because of restrictions typical for spatial structure of $GeSe_{4/2}$ tetrahedra [2], whole glassy network cannot be built by CS and/or ES clusters solely, but rather

mixed interconnecting ES-CS ones. The CS units are needed to close the ES tetrahedra in Ge-Se ChG within more stretched ORR structural motives [16]. This conclusion is argued by good agreement with known experimental data on chemical ordering in Ge-Se ChG using high-resolution XPS measurements [21].

4. Conclusions

Topological configurations of principal network-forming clusters in trigonal-type As-Se and tetragonal-type Ge-Se glasses are examined using CINCA modeling. Three different types of principal network-forming clusters and corresponding intra-cluster cores between neighboring polyhedrons composing these glasses (corner-, edge- and face-sharing trigonal $AsSe_{3/2}$ pyramids and $GeSe_{4/2}$ tetrahedrons) have been studied. It is shown that corner-sharing configurations with one common atom in direct interlinking bridge are evidently preferential for $AsSe_{3/2}$ pyramids in As-Se glasses, while corner- and edge-sharing configurations (with one and two common Se atoms, respectively) are almost equivalent in their forming energies for $GeSe_{4/2}$ tetrahedra in Ge-Se glasses. The reason for such difference in network-forming tendencies in these ChG is angular distortion within intra-cluster cores corresponding to interlinked $AsSe_{3/2}$ pyramidal and $GeSe_{4/2}$ tetrahedral building blocks.

Acknowledgements

References

[1] Z.U. Borisova, Glassy Semiconductors, Plenum Press, New York (1981).

[2] A. Feltz, Amorphous inorganic materials and glasses, Weinheim, Basel, Cambridge, New York, NY, VCH (1993).

[3] J.-L. Adam, X. Zhang (Eds.), Chalcogenide glasses: Preparation, properties and applications, Woodhead Publ. Ser. in Electronics and Optical Materials, Philadelphia-New Delhi, 2013.

[4] J. S. Sanghera, I. D. Aggarwal, J. Non-Cryst. Sol. **256-257**, 6 (1999).

[5] B. Bureau, X. Zhang, F. Smektala, J.-L. Adam, J. Troles, H. Ma, C. Boussard-Pledel, J. Lucas, P. Lucas, D. Le Coq, M. R. Riley, J. H. Simmons, J. Non-Crys. Sol. **345-346**, 276 (2004).

[6] X. Zhang, B. Bureau, P. Lucas , C. Boussard-Pledel, J. Lucas, Chem. Eur. J., **14**, 432 (2008).

[7] H. Tao, X. Zhao, Q. Liu, J. Non-Cryst. Sol. **377**, 146 (2013).

[8] K. Tanaka, J. Mater. Sci.: Mater. Electron. **16,** 633 (2005).

[9] S. Charnovych, N. Dmitruk, I. Voynarovych, N. Yurkovich, S. Kokenyesi, Plasmonics **7**, 341 (2012).

[10] M. B. Myers, E. J. Felty, Mat. Res. Bull. **2,** 535 (1967).

[11] B. Bureau, J. Troles, M. Le Floch, F. Smektala, J. Lucas, J. Non-Cryst. Solids **326-327**, 58 (2003).

[12] B. Bureau, J. Troles, M. LeFloch, F. Smektala, G. Silly, Solid State Sci. **5**, 219 (2003).

[13] O. Shpotyuk, M. Hyla, V. Boyko, Comp. Mat. Sci. **110**, 144 (2015).

[14] R. Golovchak, B. Bureau, O. Shpotyuk, V. Boyko, M. Hyla, J. Non-Cryst. Solids **377**, 43 (2013).

[15] M. Deschamps, C. Roiland, B. Bureau, G. Yang, L. Le Polles, D. Massiot, Solid State Nuclear Magnetic Resonance **40**, 72 (2011).

[16] P. M. Bridenbaugh, G. P. Espinosa, J. E. Griffiths, J. C. Phillips, J. P. Remeika, Phys. Rev. B **20**, 4140 (1979).

[17] O. Shpotyuk, R. Golovchak, V. Boyko, S. Kozyukhin, Phys. Stat. Sol. C **7**, 921 (2010).

[18] O. Shpotyuk, R. Golovchak, V. Boyko, M. Hyla, J. Non-Cryst. Sol. **357**, 479 (2011).

[19] O. Shpotyuk, R. Golovchak, Phys. Stat. Sol. C **8**, 2572 (2011).

[20] O. Shpotyuk, R. Golovchak, J. Optoelectron. Adv. M. **14**, 596 (2012).

[21] R. Golovchak, O. Shpotyuk, S. Kozyukhin, A. Kovalskiy, A.C. Miller, H.J. Jain, J. Appl. Phys. **105,** 103704-1 (2009).

[22] J. C. Phillips, J. Non-Cryst. Sol. **34**, 153 (1979).

[23] M. F. Thorpe, J. Non-Cryst. Sol. **57**, 355 (1983).

[24] G. Dittmar, H. Schäfer, Acta Cryst. **B32**, 1188 (1976).

[25] O. Shpotyuk, M. Hyla, V. Boyko, J. Optelectron. Adv. M. **15**, 1429 (2013).

[26] O. Shpotyuk, V. Boyko, M. Hyla, Phys. Stat. Sol. C **6**, 1882 (2009).

[27] R. L. Myuller, Solid state chemistry and glassy state. Ed. Leningr. Univ., 1965. P. 9-63.

[28] J. C. Mauro, A. K. Varshneya, J. Non-Cryst. Sol. **353**, 1226 (2007).

[29] M. Bauchy, M. Micoulaut, J. Non-Cryst. Sol. **377**, 34 (2013).

[30] M. Cobb, D.A. Drabold, R. L.Capelletti, Phys. Rev. B **54**, 12162 (1996).

[31] F. Inam, M. T. Shatnawi, D. Tafen, S. J. L. Billinge, P. Chen, D. A. Drabold, J. Phys.: Condens. Matter. **19**, 455206-1 (2007).

[32] W. J. Hehre, R. F. Stewart J. A. Pople, J. Chem. Phys. **51**, 2657 (1969).

[33] A. D. McLean, G. S. Chandler, J. Chem. Phys. **72**, 5639 (1980).

[34] A. L. Renninger, B. L. Averbach, Acta Cryst. B **29**, 1583 (1973).

[35] J. C. Phillips, C. A. Beevers, S. E. B. Gould, Phys. Rev. B **21**, 5724 (1980).

[36] A. L. Renninger, B. L. Averbach, Phys. Rev. B **8**, 1507 (1973).

[37] A. J. Leadbetter, A. J. Apling, J. Non-Cryst. Sol. **15**, 250 (1974).

[38] L. Pauling, The nature of the chemical bond, III ed. Oxford Univ. Press, London, (1959).

[39] R. Golovchak, A. Kovalskiy, A. Miller, H. Jain, O. Shpotyuk, Phys. Rev. **B76**, 125208 (2007).

[40] A. Ingram, A. Kozdras, O. Shpotyuk, R. Golovchak, Phys. Stat. Sol., **B249**, 1017 (2012).

[41] G. Dittmar, H. Schäfer, Die Kristallstructur von Germaniumdiselenid, Acta Cryst. B **32**, 2726 (1976).

[42] I. Petri, P. S. Salmon, H. E. Fischer, Phys. Rev. Lett. **84**, 2413 (2000).

[43] P. S. Salmon, J. Non-Cryst. Sol. **353**, 2959 (2007).

[44] P. S. Salmon, J. Phys.: Condens. Matter **19**, 455208-1 (2007).

[45] Y. Murakami, T. Usuki, M. Sakurai, S. Kohara, Mat. Sci. Eng. A **449-451**, 544 (2007).

[46] V. Petkov D. Qadir, S.D. Shastri, Sol. State Comm. **127**, 239 (2004).

[47] A. Okazaki, J. Phys. Soc. Jap. **13**, 1151 (1958).

[48] H. Wiedemeier, H.G. Schnering, Z. Kristallogr. **148**, 295 (1978).

[49] Y. Shirakawa, T. Matsuda, Y. Tani, A. Shimosaka, J. Hidaka, J. Non-Cryst. Sol. **293-295**, 764 (2001).

[50] T. Usuki, F. Araki, O. Uemura, Y. Kameda, T. Nasu, M. Sakurai, Mater. Trans. **44**, 344 (2003).

_____
*Corresponding author: olehshpotyuk@yahoo.com